Chemical Communications

COMMUNICATION

Ion Flow in a Zeolitic Imidazolate Framework Results in Ionic Diode Phenomena

Elena Madrid,[a] Mark A. Buckingham,[a] James M. Stone,[b] Adrian T. Rogers,[c] William J. Gee,[a] Andrew D. Burrows,[a] Paul R. Raithby,[a] Veronica Celorrio,[d] David J. Fermin,[d] and Frank Marken*[a]

Ionic transport (for applications in nanofluidics or membranes) and "ionic diode" phenomena in a zeolitic imidazolate framework (ZIF-8) are investigated by directly growing the framework from aqueous Zn^{2+} and 2-methylimidazole as an "asymmetric plug" into a 20 μm diameter pore in a ca. 6 μm thin poly-ethylene-terephthalate (PET) film.

Zeolitic imidazolate frameworks have been developed as an exceptionally stable (in organic and alkaline media) and versatile group of materials[1,2] with applications ranging from gas storage[3] to photocatalysis,[4] catalysis,[5] and biosensors.[6] The transformation of ZIF-8 into photo-active ZnO nano-rods has been observed.[7] Growth of ZIF-8 type materials on substrates such a silicon wafers,[8,9] glass,[10] and polymer supports[11] has been reported.

There is considerable interest in proton[12] and low temperature ion[13] conductivity in ZIF-type materials for potential applications in battery, energy storage, and sensor technologies. Reliable measurements of ion transport in ZIF-type materials provide a challenge and are often hampered for example due to grain boundary effects. Therefore, here a ZIF-8 "plug" (see Figure 1) with well-defined diameter and length is grown directly into a PET substrate with a 20 μm diameter hole. Ion transport phenomena are investigated and "ionic diode" or ion current rectification effects are observed. Ionic diode phenomena (see for example "iontronics"[14] and biomimetic pore processes[15]) in microporous materials are of interest for a wider range of applications including switchable membranes,[16] nucleic acid detection[17] and desalination.[18]

a. Department of Chemistry, University of Bath, Bath BA2 7AY, UK, Email F.Marken@bath.ac.uk
b. Centre for Photonics and Photonic Materials, Department of Physics, University of Bath, Bath BA2 7AY, UK
c. Address here. Microscopy and Analysis Suite, Department of Physics, University of Bath, Bath BA2 7AY, UK
d. School of Chemistry, University of Bristol, Bristol, BS8 1TS, UK
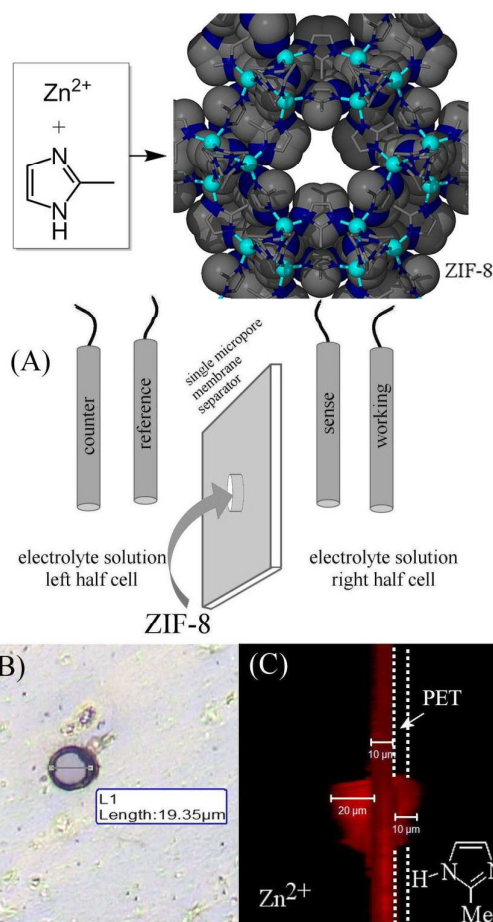
Figure 1. Reaction scheme for ZIF-8 growth from zinc(II) and 2-methylimidazole. (A) Schematic drawing of the 4-electrode configuration with PET film containing a ZIF-8-filled pore. (B) Optical microscope image of the open pore. (C) Fluorescence images for eosin Y stained ZIF-8 in side view.

Growth of microporous ZIF-8 materials directly from aqueous solution[19] is possible at room temperature‡.[20] ZIF-8 based on zinc(II) and 2-methylimidazolate exhibits a sodalite

(SOD) topology with a typical pore cavity of 11.6 Å and a pore aperture of 3.4 Å (defined as the largest sphere diameter to fit into the open space in the structure contacting the internal van der Waals surfaces).[1] It has been shown that a porous Nylon film[21] separating solutions of Zn^{2+} and 2-methylimidazole can be used to grow thin films of ZIF-8. In a similar manner, here a PET film with a single 20 μm diameter laser-drilled pore (see Figure 1B) is employed to grow ZIF-8 and to investigate ionic transport.

Growth of ZIF-8 is observed when placing the open pore PET film between aqueous solutions of 0.01 M $Zn(NO_3)_2$ and 0.7 M 2-methylimidazole. The growth is initially rapid (as seen by optical microscopy) and then progresses more slowly. The product growing in the pore shows Raman features consistent with ZIF-8 powder samples (see Figure SI1). After 48 h growth time a ZIF-8 sample was stained with eosin Y (a negatively charged dye dissolved in water-ethanol 50:50 to bind to the ZIF-8 framework at positive surface sites; XRD data for independently prepared ZIF-8 powder before and after eosin Y staining are presented in Figure SI2) and investigated by fluorescence imaging (Figure 1C). In addition to the ZIF-8 plug a film of ZIF-8 formed on the zinc(II) solution side. Also the most extended ZIF-8 growth occurs on the zinc(II) solution side. These observations suggest slow ingress of 2-methylimidazol and transport through the organic PET film followed by reaction at the Zn^{2+} side as the main growth mechanism. Direct transport through the ZIF-8 seems inefficient and slower compared to permeation through PET perhaps due to blockage. The resulting ZIF-8 plug is approximately 20 μm in diameter. When investigating the electron optical images for the ZIF-8 growth, distinct appearances for the zinc(II) side and the 2-methylimidazole side (Figure 2) are seen. The main growth is present on the zinc(II) side, but the growth appears to progress from the perimeter with 2-methylimidazole transport through PET rather than directly through the ZIF-8.
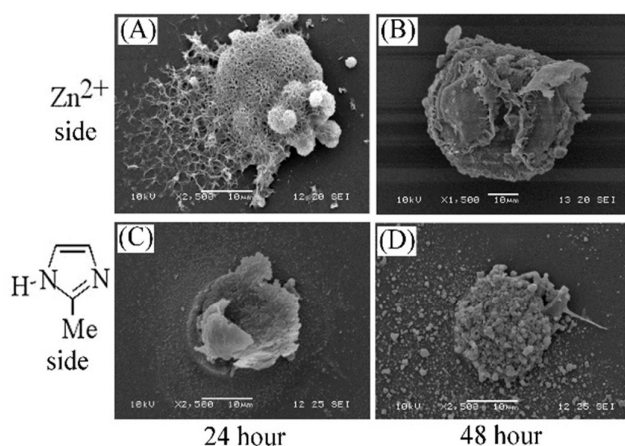

Figure 2. SEM images for the growth of ZIF-8 shown from the zinc(II) side and from the 2-methylimidazole side for 24 h and for 48 h growth.

Electrochemical studies close to equilibrium with low applied bias voltages confirmed the presence of the ZIF-8 deposit. Impedance measurements (4-electrode, open circuit, 25 mV amplitude, 1 to 10^5 Hz, see Figure SI3) in aqueous $NaNO_3$ revealed (apart from the PET film capacitance and the solution resistance components) a resistive element associated with the pore. In 1 mM $NaNO_3$ | 1 mM $NaNO_3$ the empty pore exhibits 3.2 MOhm resistance and when filled with ZIF-8 this goes up to 6.9 MOhm. In 10 mM $NaNO_3$ | 10 mM $NaNO_3$ and higher concentration solution the resistance for the open pore and the ZIF-8-filled pore become more similar. These results suggest good ion mobility with a strong effect of ionic strength. For concentrations of $NaNO_3$ higher than 0.1 M the ZIF-8 "plug" became unstable and sometimes was removed from the PET hole during experiments. This is likely to result from a lack of adhesion between ZIF-8 and the thin PET frame.

Cyclic voltammetry experiments with higher applied bias voltages were studied next. Figure 3A shows data for a ZIF-8-filled pore in 10 mM NaOH | 10 mM NaOH with data for the open pore (dashed line) superimposed. The ZIF-8-filled pore shows good ion conductivity with some additional features at +2V. When employing 10 mM HNO_3 | 10 mM NaOH a new characteristic is observed (Figure 3B). Cyclic voltammograms are observed to "stabilise" towards a steady state over the first 5 potential cycles (see Figure SI4) indicative of some structural changes under these conditions. In contrast to the open pore behaviour (dashed line) the ZIF-8-filled pore shows strong current rectification. Note that the current for the "open diode" is also enhanced when compared to the open pore. The experiment was repeated with 48 h growth (Figure 3C) and 72 h growth (Figure 3D). Similar "ionic diode" behaviour was reported recently for polymers of intrinsic microporosity[16] and attributed to the formation of a resistive ion annihilation zone where protons and hydroxide combine (see schemes in Figure 3F and G).

In order to obtain further information about the switching time of the "ionic diode", chronoamperometry data were recorded (Figure 3E). Short transient current features are seen when switching from closed to open state and in particular when switching from open to closed. The time constant, ca. 0.5 s, is indicative of rapid ion movement across the ZIF-8 plug (consistent with the aqueous diffusion time typical for ion transport across 20 μm). The estimated charge under the transient peak, ca. 250 nC (at 20 s), can be compared to the number of ions in a volume consistent with the ZIF-8 plug and for 10 mM solution, equivalent to only ca. 6 nC. This suggests that surface charges in ZIF-8 are dominating and a higher concentration of mobile anions is present within the ZIF-8 interior approximately consistent with one anion per Zn^{2+}, as reported recently based on tri-iodide adsorption data reported for ZIF-8.[22]

ChemComm Accepted Manuscript

damaged the ZIF-8 "plug". The type of charge transporting ion (or mechanism) has so far not been identified. Future device improvements are possible for arrays of "plugs" (for example in micro-structured substrates) and for ZIF-type materials engineered for improved robustness and adhesion. The observation of "ionic diode" behaviour could be of interest due to (i) the low current or the high current region (the "closed/open diode") offering a novel analytical tool for example for poly-anions and (ii) the high current (the "open diode") exceeding the current for the open pore, effectively accelerating ionic transport through the pore. This may be attributed to an elevated concentration of mobile ions localised within the ZIF-8 plug enhancing local migration contributions. Further qualitative and quantitative study and analysis of phenomena associated with ion flow in ZIF-8 will be required. Rectification phenomena are of potential future use in energy harvesting[23] and in nanofluidic ion pumps.[24] Further study with a wider range of ions and conditions and with other ZIF materials will be necessary.

Notes and references

‡ *Chemical Reagents*. Sodium hydroxide, concentrated nitric acid (>69.0%), sodium nitrate (99.0%), 2-methylimidazole (99%) and eosin-Y were purchased from Sigma-Aldrich and zinc nitrate hexahydrate (98%) from ACROS. PET films were either supplied by Laser Micromachining Limited, St. Asaph, Denbighshire LL17 0JG UK, or purchased from Goodfellow, UK. Ultra-pure water, with 18.2 MΩ cm was supplied by an ELGA Purelab Classic system and used in all electrolyte solutions.

Instrumentation and Procedures. Electrochemical properties of the single 20 μm pore in a PET membrane were studied using an Eco Chemie Autolab PGSTAT12 potentiostat controlled with GPES 4.7 software in 4-electrode configuration. A potential was applied through two Pt wires with KCl-saturated calomel sensor and reference electrodes. For growth of the ZIF-8 "plug", equal volumes of 0.7 M 2-methylimidazole and 0.01 M $Zn(NO_3)_2$ were poured in the left and right side of an H-cell with the PET film flanged in the middle. Once the ZIF had grown the growth solutions were removed by decantation, and the PET film was washed with deionised water and dried in air.

For fluorescence analysis, eosin Y (0.1 mM in 50:50 ethanol-water) solution with the ZIF-8 membrane immersed for two days. Laser Scanning Confocal system (Carl Zeiss LSM510Meta) with an inverted microscopy based on an Axiovert 200M was used to map ZIF-8 material on the membrane and within the pore when eosin Y was excited using a HeNe laser at 543nm 30%. The images were adjusted using Zeiss LSM v 4.2 software. Scanning electron microscopy (SEM) images were obtained using a JEOL FESEM6301F microscope.
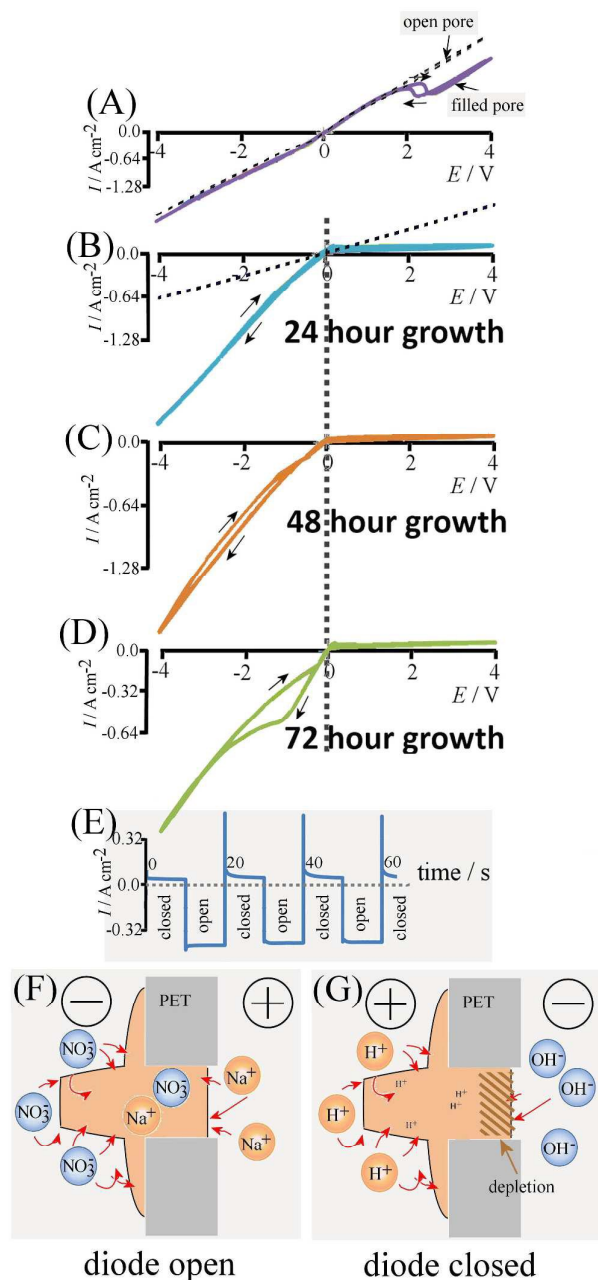
Figure 3. (A) Cyclic voltammograms (5th cycle, 24 h growth, scan rate 20 mV s⁻¹) in 10 mM NaOH | 10 mM NaOH comparing an open pore (dashed line) and a ZIF-8-filled pore. (B) Cyclic voltammograms (24 h growth) in 10 mM NaOH | 10 mM HNO₃ comparing an open pore (dashed line) and a ZIF-8-filled pore. (C) As above for 48 h growth. (D) As above for 72 h growth. (E) Chronoamperometry data for 72 h growth switching the applied potential between +/-2 V. Current data scaled assuming a pore area of 3.14 × 10⁻⁶ cm². (F,G) Schematic drawings depicting the proposed "ionic diode" mechanism.

In conclusion, it has been shown that facile ion transport is possible through a ZIF-8 "plug", in particular at 10 mM ionic strength levels. Higher ionic strength solutions irreversibly

ChemComm Accepted Manuscript

1 K.S. Park, Z. Ni, A.P. Cote, J.Y. Choi, R.D. Huang, F.J. Uribe-Romo, H.K. Chae, M. O'Keeffe and O.M. Yaghi, *PNAS*, 2006, **103**, 10186.

2 A. Phan, C.J. Doonan, F.J. Uribe-Romo, C.B. Knobler, M. O'Keeffe and O.M. Yaghi, Acc. Chem. Res., 2010, 43, 58.

3 P.F. Cheng and Y.H. Hu, *J. Phys. Chem. C*, 2014, **118**, 21866.

4 H.P. Jing, C.C. Wang, Y.W. Zhang, P. Wang and R. Li, *RSC Adv*., 2014, **4**, 54454.

5 R.Z. Jin, Z. Bian, J.Z. Li, M.X. Ding and L.X. Gao, *Dalton Trans.,* 2013, **42**, 3936.

6 W.J. Ma, Q. Jiang, P. Yu, L.F. Yang and L.Q. Mao, *Anal. Chem.*, 2013, **85**, 7550.

7 L.H. Wee, N. Janssens, S.P. Sree, C. Wiktor, E. Gobechiya, R.A. Fischer, C.E.A. Kirschhock and J.A. Martens, *Nanoscale*, 2014, **6**, 2056.

8 S. Eslava, L.P. Zhang, S. Esconjauregui, J.W. Yang, K. Vanstreels, M.R. Baklanov and E. Saiz, *Chem. Mater*., 2013, **25**, 27.

9 G. Lu, O.K. Farha, W.N. Zhang, F.W. Huo and J.T. Hupp, *Adv. Mater.*, 2012, **24**, 3970.

10 G. Lu and J.T. Hupp, *J. Am. Chem. Soc.*, 2010, **132**, 7832.

11 Y.B. Li, L.H. Wee, A. Volodin, J.A. Martensa and I.F.J. Vankelecom, *Chem. Commun.*, 2015, **51**, 918.

12 P. Barbosa, N.C. Rosero-Navarro and F.M.L. Figueiredo, *Electrochim. Acta*, 2015, **153**, 19.

13 K. Fujie, K. Otsubo, R. Ikeda, T. Yamada and H. Kitagawa, *Chem. Sci.*, 2015, **6**, 4306.

14 H.G. Chun and T.D. Chung, *Ann. Rev. Anal. Chem.*, 2015, **8**, 441.

15 W. Guo, Y. Tian and L. Jiang, *Acc. Chem. Res*., 2013, **46**, 2834.

16 E. Madrid, Y.Y. Rong, M. Carta, N.B. McKeown, R. Malpass-Evans, G.A. Attard, T.J. Clarke, S.H. Taylor, Y.T. Long and F. Marken, *Angew. Chem. Inter. Ed*., 2014, **53**, 10751.

17 Y.F. Liu and L. Yobas, *Biosens. Bioelectronics*, 2013, **50**, 78.

18 E. Madrid, P. Cottis, Y.Y. Rong, A.T. Rogers, J.M. Stone, R. Malpass-Evans, M. Carta, N.B. McKeown and F. Marken, *J. Mater. Chem. A*, 2015, **3**, 15849.

19 Y.C. Pan, Y.Y. Liu, G.F. Zeng, L. Zhao and Z.P. Lai, *Chem. Commun.*, 2011, **47**, 2071.

20 M.P. Jian, B. Liu, R.P. Liu, J.H. Qu, H.T. Wang and X.W. Zhang, *RSC Adv.*, 2015, **5**, 48433.

21 M. He, J.F. Yao, L.X. Li, Z.X. Zhong, F.Y. Chen and H.T. Wang, *Micropor. Mesopor. Mater*., 2013, **179**, 10.

22 X.X. Fan, W. Wang, W. Li, J.W. Zhou, B. Wang, J. Zheng and X.G. Li, *ACS Appl. Mater. Interf.*, 2014, **6**, 14994.

23 J. Gao, W. Guo, D. Feng, H.T. Wang, D.Y. Zhao and L. Jiang, *J. Amer. Chem. Soc.*, 2014, **136**, 12265.

24 H.C. Zhang, X. Hou, L. Zeng, F. Yang, L. Li, D.D. Yan, Y. Tian and L. Jiang, *J. Amer. Chem. Soc.*, 2013, **135**, 16102.

Graphical Abstract